Acta Oceanol. Sin., 2016, Vol. 35, No. 8, P. 89–98
DOI: 10.1007/s13131-016-0880-3
http://www.hyxb.org.cn
E-mail: hyxbe@263.net

Green synthesis of iron oxide (Fe_3O_4) nanoparticles using two selected brown seaweeds: Characterization and application for lead bioremediation

EL-KASSAS Hala Y.[1]*, ALY-ELDEEN Mohamed A.[1], GHARIB Samiha M.[1]

[1] National Institute of Oceanography and Fisheries, Alexandria 21556, Egypt

Received 17 June 2015; accepted 28 August 2015

©The Chinese Society of Oceanography and Springer-Verlag Berlin Heidelberg 2016

Abstract

The exploitation of different plant materials for the biosynthesis of nanoparticles is considered a green technology because it does not involve any harmful chemicals. In this study, iron oxide nanoparticles (Fe_3O_4-NPs) were synthesized using a completely green biosynthetic method by reduction of ferric chloride solution using brown seaweed water extracts. The two seaweeds *Padina pavonica* (Linnaeus) Thivy and *Sargassum acinarium* (Linnaeus) Setchell 1933 were used in this study. The algae extract was used as a reductant of $FeCl_3$ resulting in the phytosynthesis of Fe_3O_4-NPs. The phytogenic Fe_3O_4-NPs were characterized by surface plasmon band observed close to 402 nm and 415 nm; the obtained Fe_3O_4-NPs are in the particle sizes ranged from 10 to 19.5 nm and 21.6 to 27.4 nm for *P. pavonica* and *S. acinarium*, respectively. The strong signals of iron were reported in their corresponding EDX spectra. FTIR analyses revealed that sulphated polysaccharides are the main biomolecules in the algae extracts that do dual function of reducing the $FeCl_3$ and stabilizing the phytogenic Fe_3O_4-NPs. The biosynthesized Fe_3O_4-NPs were entrapped in calcium alginates beads and used in Pb adsorption experiments. The biosynthesized Fe_3O_4-NPs alginate beads via *P. pavonica* (Linnaeus) Thivy had high capacity for bioremoval of Pb (91%) while that of *S. acinarium* (Linnaeus) Setchell 1933 had a capacity of (78%) after 75 min. The values of the process parameters for the maximum Pb removal efficiency by Fe_3O_4-NPs alginate beads synthesized *via P. pavonica* (Linnaeus) Thivy were also estimated.

Key words: seaweeds, iron oxide, silver, nanoparticles

Citation: El-Kassas Hala Y, Aly-Eldeen Mohamed A, Gharib Samiha M. 2016. Green synthesis of iron oxide (Fe_3O_4) nanoparticles using two selected brown seaweeds: Characterization and application for lead bioremediation. Acta Oceanologica Sinica, 35(8): 89–98, doi: 10.1007/s13131-016-0880-3

1 Introduction

During last two decades, extensive attention has been paid on the management of environmental pollution caused by hazardous materials. Contamination by heavy metals is a growing global problem as they are non-biodegradable and thus persistent. Metals are mobilized and carried into food web as a result of leaching from waste dumps, polluted soils and water. For this motive, many techniques for environmental remediation of heavy metals are being studied (Ofer et al., 2003; Bayramoğlu et al., 2006; Rai, 2008, 2010; Rawat et al., 2011). Lead being one of the "big three" toxic heavy metals because it is rapidly accumulated by organisms including fish (Ribeiro et al., 2010) and becomes concentrated throughout the food chain to humans (ATSDR, 2001; Crist et al., 1992).

Recently, macroalgae have been increasingly used as a tool for monitoring marine environments contaminated by heavy metals (Daka et al., 2003; Stengel et al., 2004; Daby, 2006; Baumann et al., 2009; Kumar et al., 2009; Tonon et al., 2011). Many macroalgae are able to accumulate high levels of trace metals, which are sometimes larger than those found in water samples from the same site (Cardwell et al., 2002; Salgado et al., 2006) and also have the ability to produce phytochemicals of potential interest (El Maghraby and Fakhry, 2015).

Bioremediation is one of the most viable options for remediating water contaminated by organic and inorganic compounds considered detrimental to environmental health. Bioremediation is a process defined as the use of microorganisms/plants to detoxify or remove organic and inorganic xenobiotics from the environment (Philp and Atlas, 2005). It is a remediation option that offers green technology solution to the problem of hydrocarbon and heavy metals contamination. Bioremediation can deal with lower concentration of contaminants where the cleanup by physical or chemical methods would not be feasible. This process offers a cost effective remediation technique, compared to other remediation methods, because it is a natural process and does not usually produce toxic by-products. It also provides a permanent solution as a result of complete mineralization of the contaminants in the environment (Perelo, 2010). Biosynthesis of different metallic nanoparticles may be triggered by several compounds that are present in marine algae (Mubarak Ali et al., 2011; Schröfel et al., 2011; Vivek et al., 2011; Rajesh et al., 2012; Asmathunisha and Kathiresan, 2013). Green nanotechnology therefore, has attracted a lot of attention and includes a wide range of processes that reduce or eliminate toxic substances to restore the environment (Asmathunisha and Kathiresan, 2013).

Biosynthesis of iron oxide nanoparticles (Fe_3O_4-NPs) using

*Corresponding author, E-mail: halayassin12@yahoo.com

seaweeds had recently been reported, it is a simple, environmentally friendly, pollutant-free, and low-cost approach (Mahdavi et al., 2013). It is considered as a modern alternative for Fe_3O_4-NPs production (Abdul Salam et al., 2012). Nanoscale iron particles represent a new generation of environmental remediation technologies that could provide cost-effective solutions to some of the most challenging environmental cleanup problems (Zhang, 2003; Li et al., 2006).

The aims of this study were using two selected brown seaweeds namely *Padina pavonica* (Linnaeus), *Sargassum acinarium* (Linnaeus) Setchell 1933 for (1) biosynthesis of Fe_3O_4-NPs, (2) application of the biosynthesized Fe_3O_4-NPs for bioremediation of lead from aqueous solution. The present investigation is expected to shed a light on the waste water purification industry.

2 Materials and methods

2.1 *Algal sampling*

The examined biological materials in this study are the brown seaweeds belonged to two families; Dictyotaceae: *Padina pavonica* (Linnaeus) Thivy and Sargassaceae: *Sargassum acinarium* (Linnaeus) Setchell 1933. They are widely distributed along Egyptian Mediterranean Coast, especially in Alexandria coast. The selected species were collected from the rocky site near Boughaz El-Maadya and Abu-Qir Bay of Alexandria coast, Egypt (Fig. 1) during spring 2013 and were identified to species level using taxonomic keys (Aleem, 1993). The two algal species are usually abundant during the relevant collected periods.

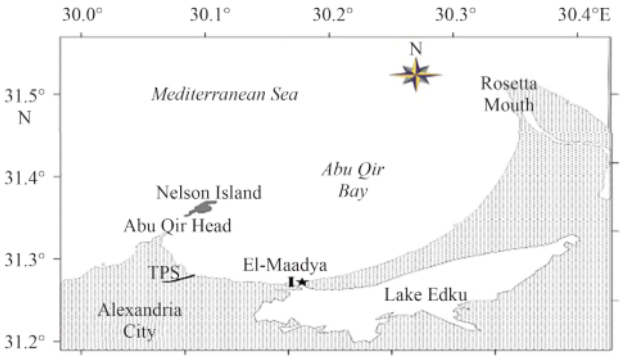

Fig. 1. Map showing Abu Qir Bay (31°19′N, 30°03′E), Egypt, where samples were collected.

2.2 *Algal extraction*

Samples of seaweeds were brought to laboratory in plastic bags containing sea water to prevent evaporation, epiphytic and extraneous matter were removed by washing first in sea water and then washed with distilled water to separate potential contaminants. All cleaned seaweeds were freeze-dried at –20°C for 3 d and then ground to fine powder using a Waring miller to pass through a 0.5-mm screen. The procedures were as follows; first, ground freeze-dried seaweed samples (about 1 g) were boiled with distilled water (100 mL) in an Erlenmeyer flask while being continuously stirred for 15 min. The extract was cooled to room temperature, filtered, and used for the biosynthesis of Fe_3O_4-NPs.

2.3 *Biosynthesis of Fe_3O_4 nanoparticles*

The magnetite (Fe_3O_4) NPs were prepared using the co-precipitation method described by Kang et al. (1996) and Qu et al (1999) with some modifications; the basic reaction is shown below:

$$2Fe^{3+} + Fe^{2+} + 8NH_3 + 4H_2O \rightarrow Fe_3O_4\,(s) + 8NH_4^+.$$

The $FeCl_3$ (0.1 mol/L) solution was added to the seaweed extract in a 1:1 volume ratio. Fe_3O_4-NPs were immediately obtained with the reduction process. The mixture was stirred for 60 min and then allowed to stand at room temperature for another 30 min. The obtained colloidal suspensions were then centrifuged and washed several times with ethanol and then dried at 40°C under vacuum to obtain the Fe_3O_4-NPs.

2.4 *Characterization of Fe_3O_4 nanoparticles*

Characterization of the biosynthesized Fe_3O_4-NPs was carried out by several processes:

2.4.1 *Infrared spectroscopy*

UV-Vis spectral analysis was performed to confirm the biosynthesis of Fe_3O_4-NPs by sampling the aqueous component and the absorption maxima was scanned by UV-Vis spectrophotometer at wavelength of 350–800 nm on Perkin-Elmer Lambda 25 spectrophotometer.

2.4.2 *Electron microscopy*

A drop (50 μL) of Fe_3O_4-NPs colloid was placed on the carbon-coated copper grids. The morphology and size analysis of the phytogenic Fe_3O_4-NPs was carried out by Transmission Electron Microscope (TEM). TEM micrographs were taken by analyzing the prepared grids on AMT Camera System. The TEM measurement of the particle sizes was done by Image Analyzer System (IAS).

2.4.3 *Energy-dispersive X-ray (EDX) microanalysis*

The structure of Fe_3O_4-NPs was characterized by Energy-dispersive X-ray (EDX) spectrum using X-ray micro-analyzer (Module Oxford 6587INCA X-sight) attached to JEOL JSM 5500 LV Scanning electron microscope to confirm the presence of iron in the particles, as well as to detect the other elementary compositions of the particles.

2.4.4 *FTIR analysis*

The biosynthesized Fe_3O_4-NPs colloid was centrifuged at 10 000 g for 15 min and the lyophilized samples were grinded with KBr pellets used for FTIR measurements. The spectrum was recorded in the range of 500–4 000 cm^{-1} using Thermo Nicolet Nexus 670 spectrometer in the diffuse reflectance mode operating at resolution of 4 cm. Spectral absorption bands were identified in relation to published information.

2.5 *Metal adsorption study*

Lead ion stock solution (1 000 mg/L) was prepared by dissolving lead nitrate (Fisher Scientific Ltd) in deionized distilled water, shaking for 15 min at 100 r/min and then left to stand for 24 h to obtain complete dissolution. Stock solution was diluted with deionized distilled water to obtain the necessary concentrations (Budavari et al., 1989). In this study the desired concentrations of Pb ranged between 75 and 175 mg/L. Solutions were adjusted to the desired pH values using diluted NaOH and diluted HNO_3. The Pb concentration was determined with an atomic absorption spectrophotometer (Unicam 929AA). Deionized water is

used during the whole work.

2.5.1 *Preparation of adsorbents*

The Fe_3O_4-NPs alginate beads were prepared by entrapping Fe_3O_4-NPs in calcium alginate beads according to the following steps: First, desired amount of Fe_3O_4-NPs was added to 10 mL of 4% (w/v) sodium alginate solution. Next, this mixture was promptly dropped into a 3.5% $CaCl_2$ solution with continuous stirring to obtain a homogeneous mixture. Finally the beads formed were allowed to harden and then rinsed with de-ionized water.

A batch equilibrium method, depending on different adsorption conditions such as contacting time, different pH, adsorbent dosage and initial lead ions concentrations, was used to determine sorption properties Fe_3O_4-NPs alginate beads. All biosorption experiments were conducted in 250 mL Erlenmeyer flasks in which biosynthesized Fe_3O_4-NPs alginate beads was exposed to metal solution at (25±2)°C on a rotary shaker at 120 r/min. After the adsorption process, the supernatant was decanted and the residual metal concentration was determined using atomic absorption spectrophotometer. All the experiments were carried out in duplicate and data presented were the mean values from these independent experiments.

The removal efficiency by the beads was calculated by the difference of initial concentration using the equation expressed as follow:

$$\text{Removal efficiency}(\%) = \frac{(C_\text{i} - C_\text{t}) \cdot 100}{C_\text{i}},$$

where C_i is initial concentration of lead (mg/L); C_t is concentration of lead (mg/L). And metal adsorbed by the biosynthesized Fe_3O_4-NPs alginate beads (metal/adsorbent, mg/g) was calculated (Volesky and May-Phillips, 1995) as

$$Q_\text{e} = V(C_\text{i} - C_\text{e})/g,$$

where Q_e is Pb uptake (Pb/adsorbent, mg/g) at equilibrium; V is the volume of liquid phase (L); C_i is initial Pb concentration (mg/L); C_e is final Pb concentration (mg/L) at equilibrium; and g is weight of adsorbent (mg).

2.5.2 *Factorial experimental design*

To evaluate the efficiency of Fe_3O_4-NPs alginate beads for adsorption of Pb from aqueous solution containing different Pb concentrations, batch adsorption experiments were conducted randomly at four different levels of independent variables coded as $+\alpha$, +1 and –1, $-\alpha$, for high and low concentrations (or values), respectively with seven central points to give a total of 31 experimental runs. The analysis focused on how the removal efficiency of lead is influenced by four independent variables namely, contact time (X_1, min), pH (X_2), adsorbent dosage (X_3, g/L), and initial lead concentration (X_4, mg/L). The low and high levels for the factors were selected according to some preliminary experiments plan outlined by fractional factorial design (El-Kassas and El-Taher, 2009). The range and levels of these independent variables investigated in this study are given in Table 1. All possible combinations of these variables were used, and a matrix was established according to their high and low levels according to Response Surface Methodology (RSM) (Table 2). For statistical calculations, the variables were coded as X_i according to the following relationship:

$$Y=\beta_0+\beta_1X_1+\beta_2X_2+\beta_3X_3+\beta_4X_4+\beta_{12}X_1X_2+\beta_{13}X_1X_3+\beta_{14}X_1X_4+\beta_{23}X_2X_3+\beta_{24}X_2X_4+\beta_{34}X_3X_4+\beta_{11}X_{21}+\beta_{22}X_{22}+\beta_{33}X_{23}+\beta_{44}X_{24},$$

Table 1. Experimental ranges and levels of independent parameters affecting Pb removal efficiency by Fe_3O_4-NP salginate beads

Independent variables	Range and level				
	$-\alpha$	–1	0	1	$+\alpha$
Time (X_1)/min	15	30	45	60	75
pH (X_2)	2	4	6	8	10
Beads dosage (X_3)/g·L^{-1}	1.25	2.5	3.75	5	6.25
Pb concentration (X_4)/mg·L^{-1}	75	100	125	150	175

Table 2. Experimental designs matrix (coded levels) of independent variables affecting Pb removal efficiency by Fe_3O_4-NPs alginate beads

Run number	X_1	X_2	X_3	X_4
1	–1	–1	–1	–1
2	1	–1	–1	–1
3	–1	1	–1	–1
4	1	1	–1	–1
5	–1	–1	1	–1
6	1	–1	1	–1
7	–1	1	1	–1
8	1	1	1	–1
9	–1	–1	–1	1
10	1	–1	–1	1
11	–1	1	–1	1
12	1	1	–1	1
13	–1	–1	1	1
14	1	–1	1	1
15	–1	1	1	1
16	1	1	1	1
17	$-\alpha$	0	0	0
18	$+\alpha$	0	0	0
19	0	$-\alpha$	0	0
20	0	$+\alpha$	0	0
21	0	0	$-\alpha$	0
22	0	0	$+\alpha$	0
23	0	0	0	$-\alpha$
24	0	0	0	$+\alpha$
25	0	0	0	0
26	0	0	0	0
27	0	0	0	0
28	0	0	0	0
29	0	0	0	0
30	0	0	0	0
31	0	0	0	0

where Y is the predicted response, β_0 is the model constant; X_1, X_2, X_3 and X_4 are independent variables; β_1, β_2, β_3 and β_4 are linear coefficients; β_{12}, β_{13}, β_{14}, β_{23}, $\beta_{24}$and β_{34} are cross product coefficients and β_{11}, β_{22}, $\beta_{33}$and β_{44} are the quadratic coefficients. The results were analyzed with Design Expert software, and the main effects and interactions between factors were determined. Experiments were performed in duplicate and results were averaged.

3 Results and discussion

Aquatic organisms are the most important biosorbents (Shanab et al., 2012). Biosynthesis of metal nanoparticles by the aquatic organisms is thought to be clean, nontoxic, and environmentally acceptable "green procedures". Seaweeds constitute

one of the commercially important marine living renewable resources (Kulkarni and Muddapur, 2014). Nanotechnology has the potential to open up new perspectives to economic, environmental and social benefits and is an innovation driver offering significant opportunities for sustainable development, growth and employment in the world (Tolles and Rath, 2003). Many microalgal species are used as biosorption of lead as the blue-green algae *Spirulina* (Chen and Pan, 2005); green algae *Scenedesmus obliquus*, *Chlorella vulgaris* and *Enteromorpha* sp. (Chekroun et al., 2014; Dwivedi, 2012; Hammud et al., 2014).

3.1 *Mechanism of the Fe_3O_4-NPs formation in algal extract*

The improvement of reliable, nontoxic, and eco-friendly methods for synthesis of nanoparticles is of utmost importance to expand their biomedical applications (Shankar et al., 2004). The present work focused on the development of a biosynthetic method for the production of Fe_3O_4-NPs using brown seaweed (*Padina pavonica* and *Sargassum acinarium*) extract. The Fe_3O_4-NPs differed from those of the noble metals such as silver (Ag-NPs) or gold (Au-NPs) in the high reactivity of iron. The Ag-NPs or Au-NPs are comparatively inert and stable and thus can be easily produced using plant extracts. However, iron ions are easily oxidized and reduced by interacting with a wide array of different chemical compounds; a factor which complicates the synthesis of stable Fe_3O_4-NPs using plant extracts (Shankar et al., 2003, 2004; Huang et al., 2007). Hence, research is focused on the preparation of novel, cheap and more effective sorbents. A very promising material, that offers such advantages, is alginate. Calcium alginate beads have also been used for the removal of Cr (VI) from aqueous solution with several types of adsorbents (Fiol et al., 2005).

In this study we will endeavor for study the production, biophysical characterization and application of the biosynthesized Fe_3O_4-NPs with the extracts of the seaweeds *P. pavonica* and *S. acinarium*. Herein, the preliminary detection of the reduction of $FeCl_3{\cdot}6H_2O$ into Fe_3O_4-NPs by the algal extractions. The color variation was obvious on visual observation from yellow to brown.

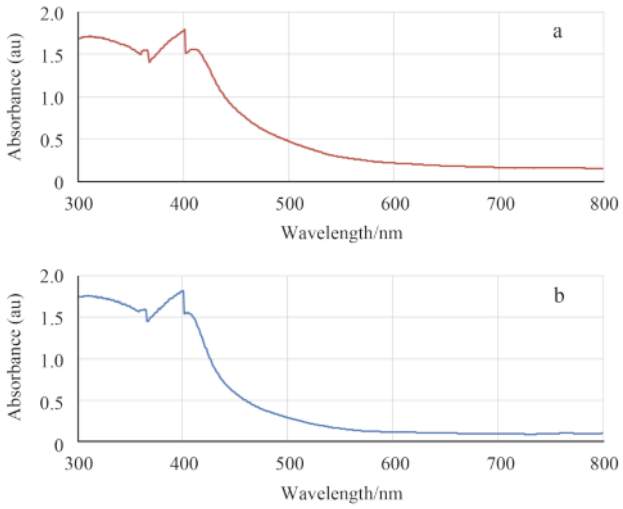

Fig. 2. UV/Vis Absorption spectrum of the capped Fe_3O_4-NPs synthesized using *Padina pavonica* (Linnaeus) Thivy (a) and *Sargassum acinarium* (b) aqueous extracts.

The brown color is due to the excitation of the surface plasmon resonance in the metal nanoparticles. In this respect, the investigation of seaweeds as possible Fe_3O_4-NPs nanofactories has been studied. And the brown color of Fe_3O_4-NPs colloid due to the formation of Fe_3O_4-NPs at the extra cellular algal levels as reported by Mahdavi et al. (2013) that was further confirmed by our TEM studies. Let alone, the biosynthesis of Fe_3O_4-NPs using *P. pavonica* and *S. acinarium* were confirmed by the UV-Vis spectral analysis at various nm as recorded in Figs 2a and b. The sharp bands that were observed close to 400 nm throughout the reaction that indicates the formation of Fe_3O_4-NPs. Furthermore and in accordance with the results of the present study, Mahdavi et al. (2013) revealed that the surface plasmon band for Fe_3O_4-NPs at wavelengths of 402 nm and 415 nm indicate the formation of iron nanoparticles. Therefore, the selected algae are very efficient in biosynthesis of Fe_3O_4-NPs.

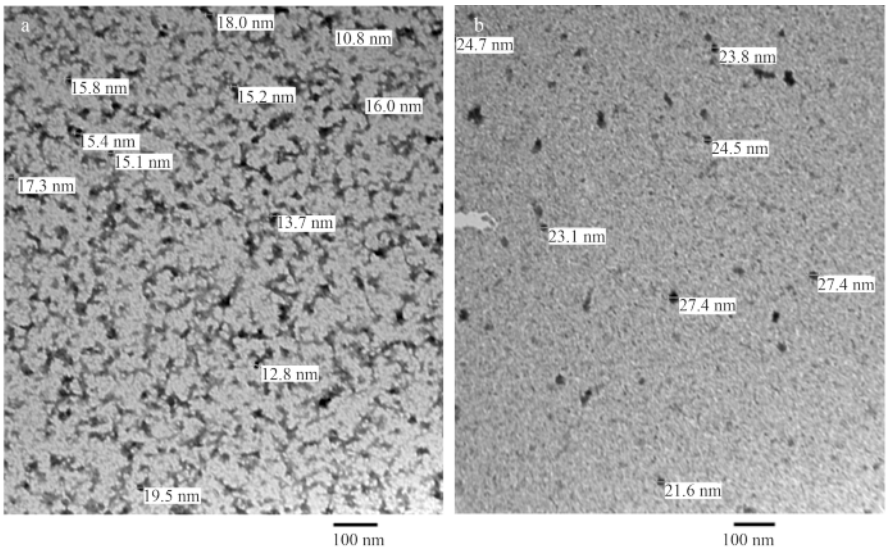

Fig. 3. Transmission electron micrographs of the capped Fe_3O_4-NPs synthesized using *Padina pavonica* (Linnaeus) Thivy (a) and *Sargassum acinarium* (b) aqueous extracts.

3.2 *Electron microscopy*

Transmission electron microscope was used in tandem for image capture of Fe_3O_4-NPs derived from *P. pavonica* and *S. acinarium* cells extract as shown in Figs 3a and b. The morphology of the nanoparticles was spherical in nature. Under careful observation, it is evident that the Fe_3O_4-NPs surrounded by a faint thin layer of other materials, which we suppose are capping organic material from seaweeds extract. The obtained Fe_3O_4-NPs are in the range of sizes 10 to 19.5 nm and 21.6 to 27.4 nm for *P. pavonica* and *S. acinarium*, respectively. Therefore, EDX measurements were used to confirm the biosynthesis of Fe_3O_4-NPs.

3.3 *EDX measurements*

The elemental composition of the two biosynthesized Fe_3O_4-NPs using *P. pavonica* and *S. acinarium* were represented in Table 3 and Figs 4a, b, respectively. The peaks around 6.39 keV are related to the binding energies of Fe in the biosynthesized Fe_3O_4-NPs colloids as reported by Dutta and Sahu (2012). Therefore, the EDX spectra for the Fe_3O_4-NPs confirmed the presence of Fe_3O_4-NPs in the two biosynthesized nano colloid.

3.4 *FTIR analyses*

The interactions between the Fe^{3+} precursor and *P. pavonica* and *S. acinarium* extracts were further confirmed by FTIR (Figs 5a and b), respectively. FTIR measurements were carried out to identify the biomolecules for capping and efficient stabilization of the Fe_3O_4-NPs synthesized via the selected seaweeds broth. FTIR spectrum of the biosynthesized Fe_3O_4-NPs via *P. pavonica* (Fig. 5a), showed that, the typical appearances of absorption spectra had three clear bands (peaks) over the wave number range 511 to 3 535 cm^{-1}. These bands in published FTIR spectra are related to specific functional groups. The week band at 3 535 cm^{-1} associated with the stretching vibrations of the OH group.

Table 3. The values of the process parameters for the maximum Pb removal efficiency by Fe_3O_4-NPs alginate beads

Parameter	Value
Q_{max}(Pb/adsorbent)/mg·g^{-1}	1 430
Pb removal efficiency/%	95.33
Pb concentration (X_4)/mg·L^{-1}	75
Fe_3O_4-NPs alginate beads (X_3)/g·L^{-1}	1.25
Equilibrium contact time (X_1)/min	15
pH (X_2)	2

The peak at 1 636 cm^{-1} correspond to protein amide I band, mainly V(C=O) stretching and may be due to the N-H bending vibration present in the carbonyl β unsaturated stretching vibration presence of Iodo compounds. Additionally, the band at 511 cm^{-1} may correspond to aliphatic iodo compounds, C-I stretch. These evidences suggested the release of protein molecules that probably had a role in the formation and stabilization of Fe_3O_4-NPs in aqueous solutions. These results of our current study complement those Dave and Chopda (2014) revealing that the presence of hydroxyl groups on the surface of Fe_3O_4-NPs provides a versatile synthetic tool to attach different functionalities. Surface modification methodologies of Fe_3O_4-NPs improved the stability and provide novel proprieties to materials. The stabilization of the Fe_3O_4-NPs is so important to produce magnetic colloidal "ferro fluids". These ferro fluids are stable against aqueous, biological medium and magnetic field. Additionally, Fig. 5b shows FTIR spectrum of Fe_3O_4-NPs synthesized using *S. acinarium*. It exhibits a number of peaks in the range of 567 to 2 065 cm^{-1}. The peak at 567 cm^{-1} is assigned to the C-H stretching vibration of CH_3. The peak at 1 637 cm^{-1} correspond to protein amide I band, mainly V(C=O) stretching and may be due to the N-H bending vibration present in the carbonyl β unsaturated-stretching vibration presence of Iodo compounds. The peak at

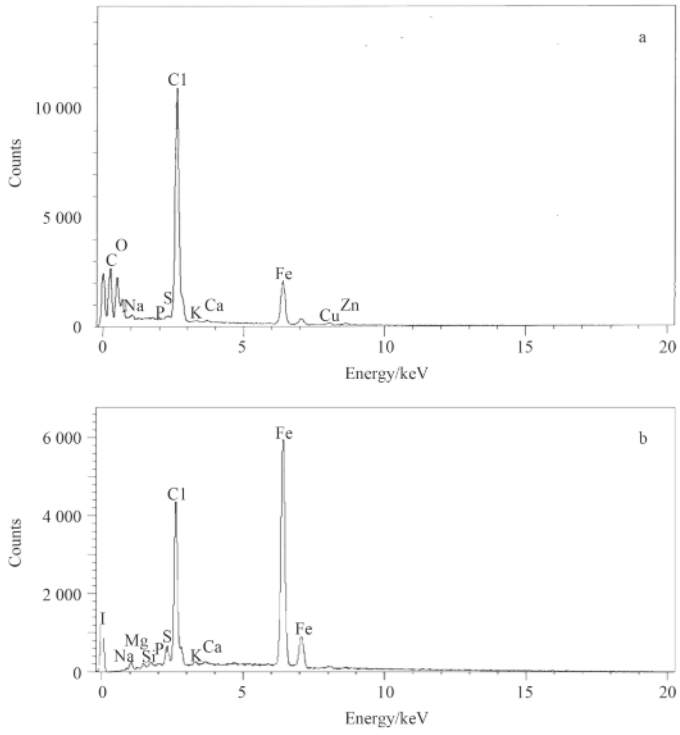

Fig. 4. EDEX spectrum of the capped Fe_3O_4-NPs synthesized using *Padina pavonica* (Linnaeus) Thivy (a) and *Sargassum acinarium* (b) aqueous extracts.

2 065 cm^{-1} is ascribed to alkyne C-C functional groups. These evidences suggested the release of protein molecules probably had a role in the formation and stabilization of Fe_3O_4-NPs in aqueous solutions. Seaweeds are well-known for their richness in several substances like lipids, minerals and certain vitamins, polysaccharides, proteins and polyphones. Thus, their phytochemicals include hydroxyl, carboxyl, and amino functional groups, which can serve both as effective metal-reducing agents and as capping agents to provide a robust coating on the metal nanoparticles (Azizi et al., 2013). Moreover, Gole et al. (2001) during their study on the biosynthesis of silver nanoparticles (Ag-NPs) stated that proteins can bind to them either through the electrostatic attraction of negatively charged carboxylate groups and therefore stabilization of the Ag-NPs by protein occurs.

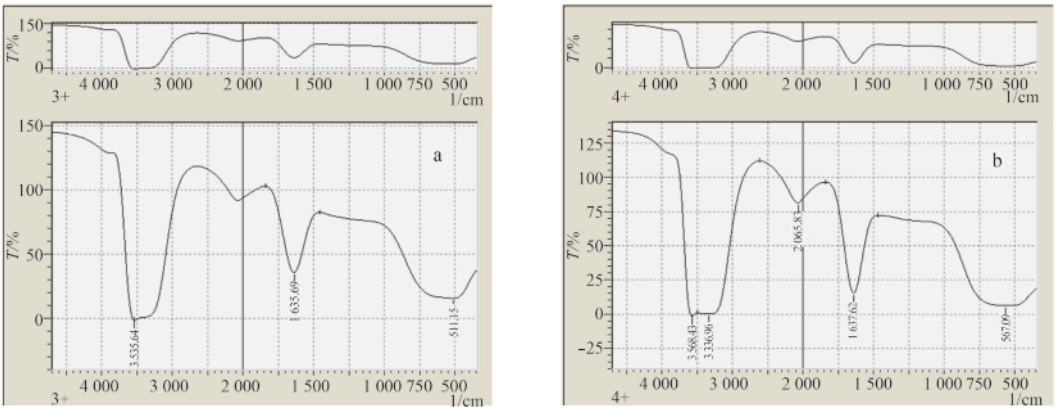

Fig. 5. FTIR spectrum of the capped Fe_3O_4-NPs synthesized using *Padina pavonica* (Linnaeus) Thivy (a) and *Sargassum acinarium* (b) aqueous extracts. *T* is transmittance (%).

3.5 *Application of the biosynthesized Fe_3O_4-NPs alginate beads*

The unique properties of nano sorbents are providing unprecedented opportunities for the removal of metals in highly efficient and cost-effective approaches, and various nanoparticles have been exploited for this purpose (Jiang et al., 2009; Afkhami and Moosavi, 2010). Nanoscale zero-valent iron has shown good potential to remove heavy metals and other aqueous pollutants (Alidokht et al., 2011; Singh et al., 2011). Recently utilization of iron oxide based nanomaterials with novel properties and functionality is widely studied due to their small size, high surface area, and magnetic property that facilitate rapid decontamination of wastewater (Laurent et al., 2008; Oh and Park, 2011).

Various physicochemical parameters namely, pH, equilibrium contact time, and adsorbent dosage as well as Pb concentra-

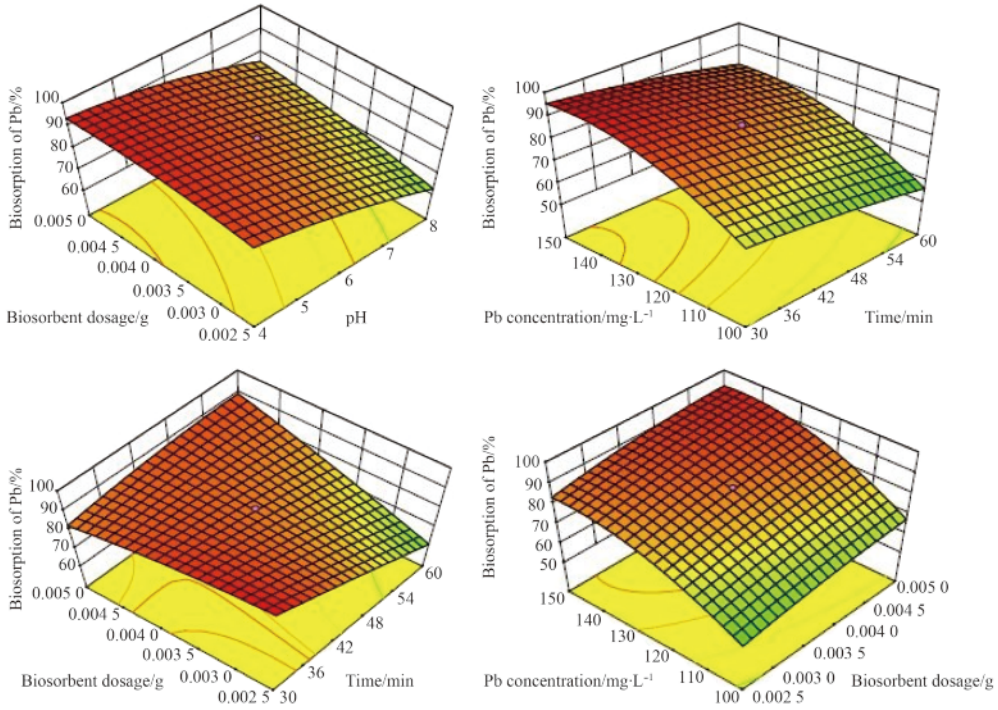

Fig. 6. Interaction effect between the different variables affecting Pb removal percentageby Fe_3O_4-NPs alginate beads synthesized using *Padina pavonica* (Linnaeus) Thivy aqueous extract as affected by the different variables.

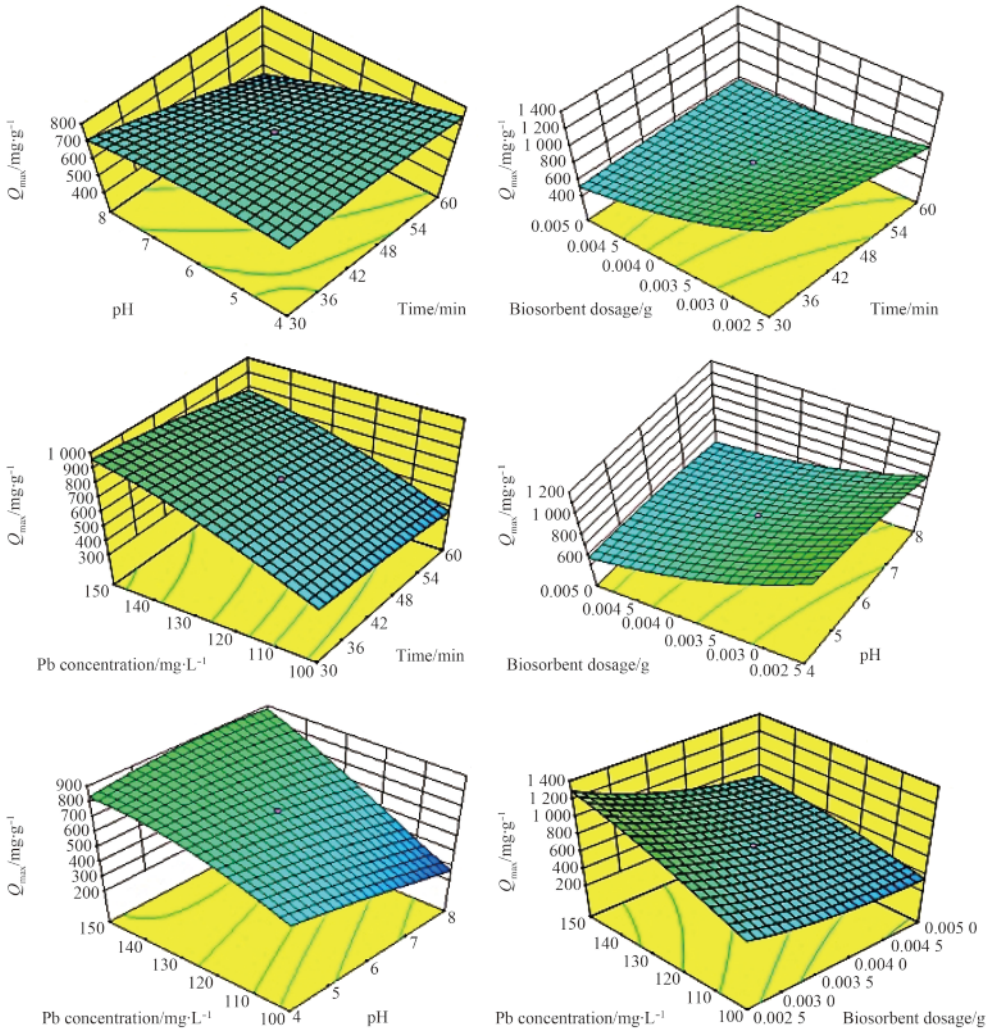

Fig. 7. Interaction effect between the different variables affecting Q_{max} by Fe_3O_4-NPs alginate beads synthesized using *Padina pavonica* aqueous extract.

tion which affect Pb adsorption have been studied. Generally, the dependence of metal sorption on pH is related to both the metal chemistry in the solution and the ionization state of the functional groups of the sorbent which affects the availability of binding sites (Ngomsik et al., 2009). In the preliminary experiments carried out by this study the biosynthesized Fe_3O_4-NPs alginate beads via *P. pavonica* and *S. acinarium* were tested for the removal of Pb from aqueous solution. Additionally the pH range and the equilibrium contact time between Fe_3O_4-NPs alginate beads and the metal solution were also evaluated.

The effect of pH ranged from 2 to 10 on the adsorption of Pb by Fe_3O_4-NPs alginate beads is studied. The adsorbent beads achieved a high Pb removal (88%, 75%) at pH 6 after 45 min for the biosynthesized Fe_3O_4-NPs alginate beads via *P. pavonica* and *S. acinarium*, respectively. The adsorption of Pb (Ⅱ) by Fe_3O_4/SiO_2-NH_2 magnetic nano-adsorbent showed maximum removal efficiency reached 89% for Pb at pH 4.0 (Mahdavi et al., 2013) and the adsorption capacity increased with increasing solution pH, while our results showed that a dramatic decrease in adsorption was observed when increasing the pH value (data not shown). In this respect Zhang et al. (2001); Mohapatra and Anand (2007) reported similar behavior during the uptake of metal ions on various adsorbents. It is widely accepted that low pH has a negative effect on metal adsorption by Fe_3O_4-NPs as indicated by Farghali et al. (2013). They revealed that at low pH, the percentage adsorption is low for metal ions, as large quantities of protons compete with metal cations for the adsorption sites. In this endeavor, Adegoke et al. (2014) during their study on Adsorption of Cr(VI) on synthetic hematite (alpha-Fe^2O^3) nanoparticles, they stated that the competition with hydroxyl ions for the adsorbent sites and the change of surface charge of the adsorbent leading to electrostatic repulsion between adsorbent and Cr(VI) anions leading to release already adsorbed ions.

The work extended to evaluate the effect of equilibrium contact time between Fe_3O_4-NPs alginate beads and the metal solution. The Fe_3O_4-NPs alginate beads succeeded to remove 91% and 78% of Pb after 75 min for the biosynthesized Fe_3O_4-NPs alginate beads via *P. pavonica* and *S. acinarium*, respectively. Again after 75 min contact time there was no further adsorption in aqueous solution containing 125 mg/L Pb using Fe_3O_4-NPs alginate beads dosage of 3.75 mg at pH 6. Similar results were recorded by Farghali et al. (2013), during their study on adsorption of Pb (Ⅱ) ions from aqueous solutions using copper oxide nanostructures. They stated that the importance of contact time comes from the need for identification of the possible rapidness of binding and removal processes of the tested metal ions by the

synthesized adsorbents and obtaining the optimum time for complete removal of the target metal ion. They added that initially all adsorbent sites were vacant and the solute concentration gradient was high. Later, Pb uptake rate by adsorbent was decreased significantly, due to the decrease in number of adsorption sites as well as Pb concentration. The biosynthesized Fe_3O_4-NPs alginate beads via *P. pavonica*, showed greater efficiency in Pb removal from the aqueous solution. Therefore it was selected to complete the optimized conditions.

3.6 *Optimization of metal uptake conditions by applying Response Surface Methodology (RSM)*

Most optimization studies during the development of a process involve variation of one factor at a time, while keeping all other factors constant. Additionally, designing the experiments using the factorial designs, enable all factors to vary simultaneously. This helps in determining the main and interactive effects of the test variables as indicated by (Khuri and Cornell, 1987; Montgomery, 1991). The statistical analyses revealed that the model is significant at 0.05% level of probability (F=6.63). In this case the main effect of pH, adsorbent dosage, Pb concentration on Pb removal and Q_{max} is significant. Similarly, the interaction effect of time and adsorbent dosage, pH and Pb concentration are significant model terms at the same level of probability(0.05%) as described in three-dimensional representations (Figs 6and 7). Using the experimental results, the model equation is

Biosorption of Pb (%) = 40.840 65–0.083 321X_1–18.527 41X_2–16.497 19X_3+1.922 35X_4–0.141 69X_1X_2+0.413 30X_1X_3–0.005 221 67×X_1X_4+0.183 75X_2X_3+0.213 34X_2X_4+0.037 340X_3X_4–0.003 477 45X_{12}–0.545 61X_{22}–0.692 75X_{32}–0.010 776X_{42}.

In addition to the pH values and equilibrium contact time previously described, the main parameter which can directly affect to the adsorption capacity of an adsorbent is the initial contaminant concentration (Ilankoon, 2014). He added, this factor must be taken into consideration when comparing the adsorption capacities of different adsorbents. The adsorbent dosage is another significant parameter in the examination of the adsorption capacity of an adsorbent. Generally, the percentage of metal removal increases with the increase of adsorbent dosage. This may be due to the availability of adsorption sites which adsorbate can get attached. The determination of effect of adsorbent dosage gives an idea about the minimum amount of adsorbent need to be used for adsorption process (Ilankoon, 2014).

The values of the process parameters for the maximum removal efficiency are shown in Table 4. These results were in close agreement with those obtained from the response surface analysis, confirming that the RSM could be effectively used to optimize the process parameters in complex processes using the statistical design of experiments. Also, the predicted values (using the model equation) were compared with experimental resultant the data are shown in Figs 8 and 9 which depicted the experimental and model predicted removal efficiencies.

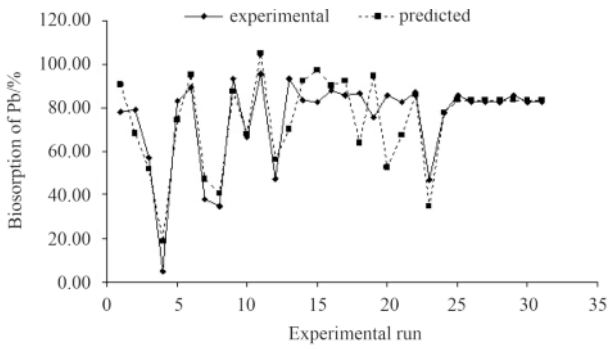

Fig. 8. Comparison between the experimental and predicted Pb removal percentageby Fe_3O_4-NPs alginate beads synthesized using *Padina pavonica* aqueous extract.

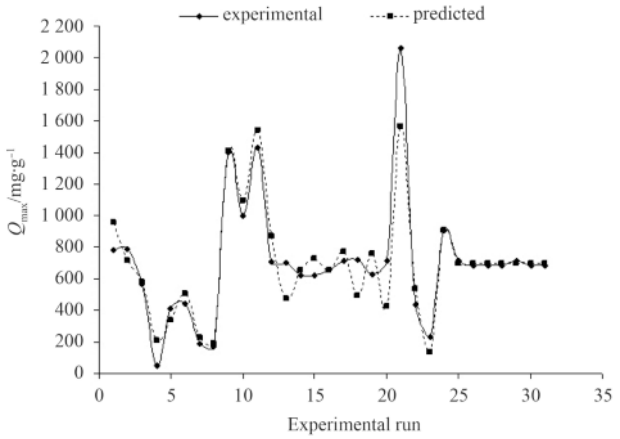

Fig. 9. Comparison between the experimental and predicted Q_{max} of Pb removal percentageby Fe_3O_4-NPs alginate beads synthesized using *Padina pavonica* aqueous extract.

4 Conclusions

Bioremediation of heavy metal pollution using the biosynthesized nanoparticles is a matter of great interest. In this study, Fe_3O_4-NPs were synthesized using a completely green biosynthetic method by reduction of ferric chloride solution with brown seaweed aqueous extract containing sulphated polysaccharides as a main factor which acts as reducing and efficient stabilizer agent. The knowledge of present study will be helpful for further assessment and management of natural algae which could serve as an economical source of treating industrial effluents with toxic metallic ions. The obtained results showed that the biosynthesized Fe_3O_4-NPs alginate beads via *P. pavonica* had high capacity for bioremoval of Pb (91%) while that of *S. acinarium* had a capacity of (78%) after 75 min.

References

Abdul Salam H, Rajiv P, Kamaraj M, et al. 2012. Plants: green route for nanoparticle synthesis. International Research Journal of Biological Science, 1(5): 85–90

Adegoke H I, AmooAdekola F, Fatoki O S, et al. 2014. Adsorption of Cr (VI) on synthetic hematite (α-Fe_2O_3) nanoparticles of different morphologies. Korean Journal of Chemical Engineering, 31(1): 142–154

Afkhami A, Moosavi R. 2010. Adsorptive removal of Congo red, a carcinogenic textile dye, from aqueous solutions by maghemite nanoparticles. Journal of Hazardous Materials, 174(1–3): 398–403

Aleem A A. 1993. Marine Algae of Alexandria. Alexandria: Privately Published

Alidokht L, Khataee A R, Reyhanitabar A, et al. 2011. Reductive removal of Cr(VI) by starch stabilized Fe^0 nanoparticles in aqueous solution. Desalination, 270(1–3): 105–110

Asmathunisha N, Kathiresan K. 2013. A review on biosynthesis of nanoparticles by marine organisms. Colloids and Surfaces B: Biointerfaces, 103: 283–287

ATSDR. 2001. Agency for toxic substances and disease registry. CERLLA Comprehensive environmental response, compensation and liability act, Priority list of hazardous substances. http://www.atsdr.cdc.gov/clist.html

Azizi S, Namvar F, Mahdavi M, et al. 2013. Biosynthesis of silver nanoparticles using brown marine Macroalga, *Sargassum Muticum* aqueous extract. Materials, 6(12): 5942–5950

Baumann H A, Morrison L, Stengel D B. 2009. Metal accumulation and toxicity measured by PAM-Chlorophyll fluorescence in seven species of marine macroalgae. Ecotoxicology and Environmental Safety, 72(4): 1063–1075

Bayramoğlu G, Tuzun I, Celik G, et al. 2006. Biosorption of mercury (Ⅱ), cadmium (Ⅱ) and lead (Ⅱ) ions from aqueous system by microalgae *Chlamydomonas reinhardtii* immobilized in alginate beads. International Journal of Mineral Processing, 81(1): 35–43

Budavari S, O'Neil M J, Smith A, et al. 1989. The Merck Index: an Encyclopedia of Chemicals, Drugs, and Biologicals. 11th ed. Rahway, NJ, USA: Merck & Co, Inc

Cardwell A J, Hawker D W, Greenway M. 2002. Metal accumulation in aquatic macrophytes from southeast Queensland, Australia. Chemosphere, 48(7): 653–663

Chekroun K B, Sánchez E, Baghour M. 2014. The role of algae in bioremediation of organic pollutants. International Research Journal of Public and Environmental Health, 1(2): 19–32

Chen Hong, Pan Shanshan. 2005. Bioremediation potential of *Spirulina*: toxicity and biosorption studies of lead. Journal of Zhejiang University Science, 6B(3): 171–174

Crist R H, Oberholser K, McGarrity J, et al. 1992. Interaction of metals and protons with algae. 3. Marine algae, with emphasis on lead and aluminum. Environmental Science and Technology, 26(3): 496–502

Daby D. 2006. Coastal pollution and potential biomonitors of metals in Mauritius. Water, Air, and Soil Pollution, 174(1–4): 63–91

Daka E R, Allen J R, Hawkins S J. 2003. Heavy metal contamination in sediment and biomonitors from sites around the Isle of Man. Marine Pollution Bulletin, 46(6): 784–791

Dave P N, Chopda L V. 2014. Application of iron oxide nanomaterials for the removal of heavy metals. Journal of Nanotechnology, 2014: Article ID 398569

Dutta R K, Sahu S. 2012. Development of oxaliplatin encapsulated in magnetic nanocarriers of pectin as a potential targeted drug delivery for cancer therapy. Results in Pharma Sciences, 2: 38–45

Dwivedi S. 2012. Bioremediation of heavy metal by algae: current and future perspective. Journal of Advanced Laboratory Research in Biology, 3(3): 195–199

El Maghraby D M, Fakhry E M. 2015. Lipid content and fatty acid composition of Mediterranean macro-algae as dynamic factors for biodiesel production. Oceanologia, 57(1): 86–92

El-Kassas H Y, El-Taher E M. 2009. Optimization of batch process parameters by response surface methodology for mycoremediation of chrome-VI by a chromium resistant strain of marine *Trichoderma viride*. American-Eurasian Journal of Agricultural & Environmental Sciences, 5(5): 676–681

Farghali A A, Bahgat M, Enaiet Allah A, et al. 2013. Adsorption of Pb (Ⅱ) ions from aqueous solutions using copper oxide nanostructures. Beni-Suef University Journal of Basic and Applied Sciences, 2(2): 61–71

Fiol N, Poch J, Villaescusa I. 2005. Grape stalks wastes encapsulated in calcium alginate beads for Cr(VI) removal from aqueous solutions. Separation Science and Technology, 40(5): 1013–1028

Gole A, Dash C, Ramakrishnan V, et al. 2001. Pepsin-gold colloid conjugates: preparation, characterization, and enzymatic activity. Langmuir, 17(5): 1674–1679

Hammud H H, El-Shaar A, Khamis E, et al. 2014. Adsorption studies of Lead by *Enteromorpha* algae and its silicates bonded material. Advances in Chemistry, 2014: Article ID 205459

Huang Jiale, Li Qingbiao, Sun Daohua, et al. 2007. Biosynthesis of silver and gold nanoparticles by novel sun dried *Cinnamomum camphora* leaf. Nanotechnology, 18(10): 105104

Ilankoon N. 2014. Use of iron oxide magnetic nanosorbents for Cr (VI) removal from aqueous solutions: A review Journal of Engineering Research and Applications, 4(10): 55–63

Jiang Mingqin, Wang Qingping, Jin Xiaoying, et al. 2009. Removal of Pb (Ⅱ) from aqueous solution using modified and unmodified kaolinite clay. Journal of Hazardous Materials, 170(1): 332–339

Kang Y S, Risbud S, Rabolt J F, et al. 1996. Synthesis and characterization of nanometer-size Fe_3O_4 and γ-Fe_2O_3 particles. Chemistry of Materials, 8(9): 2209–2211

Khuri A I, Cornell J A. 1987. Response Surfaces: Design and Analysis. New York: Marcel Dekker

Kulkarni N, Muddapur U. 2014. Biosynthesis of metal nanoparticles: a review. Journal of Nanotechnology, 2014: Article ID 510246

Kumar J I N, Oommen C, Kumar R N. 2009. Biosorption of heavy metals from aqueous solution by green marine macroalgae from Okha Port, Gulf of Kutch, India. American-Eurasian Journal of Agricultural & Environmental Sciences, 6(3): 317–323

Laurent S, Forge D, Port M, et al. 2008. Magnetic iron oxide nanoparticles: synthesis, stabilization, vectorization, physicochemical characterizations, and biological applications. Chemical Reviews, 108(6): 2064–2110

Li Xiaoqin, Elliott D W, Zhang Weixian. 2006. Zero-valent iron nanoparticles for abatement of environmental pollutants: Materials and Engineering Aspects. Critical Reviews in Solid State and Materials Sciences, 31(4): 111–122

Mahdavi M, Namvar F, Ahmad M B, et al. 2013. Green biosynthesis and characterization of magnetic iron oxide (Fe_3O_4) nanoparticles using seaweed (*Sargassum muticum*) aqueous extract. Molecules, 18(5): 5954–5964

Mohapatra M, Anand S. 2007. Studies on sorption of Cd (Ⅱ) on Tata chromite mine overburden. Journal of Hazardous Materials, 148(3): 553–559

Montgomery D C. 1991. Design and Analysis of Experiments. 3rd ed. New York: Wiley

Mubarak Ali D, Divya C, Gunasekaran M, et al. 2011. Biosynthesis and characterization of silicon-germanium oxide nanocomposite by Diatom. Digest Journal of Nanomaterials and Biostructures, 6(1): 117–120

Ngomsik A F, Bee A, Siaugue J M, et al. 2009. Co (Ⅱ) removal by magnetic alginate beads containing Cyanex 272®. Journal of Hazardous Materials, 166(2–3): 1043–1049

Ofer R, Yerachmiel A, Shmuel Y. 2003. Marine macroalgae as biosorbents for cadmium and nickel in water. Water Environment Research, 75(3): 246–253

Oh J K, Park J M. 2011. Iron oxide-based superparamagnetic polymeric nanomaterials: design, preparation, and biomedical application. Progress in Polymer Science, 36(1): 168–189

Perelo L W. 2010. Review: In situ and bioremediation of organic pollutants in aquatic sediments. Journal of Hazardous Materials, 177(1–3): 81–89

Philp J C, Atlas R M. 2005. Bioremediation of contaminated soils and aquifers. In: Atlas R M, Philp J C, eds. Bioremediation: Applied Microbial Solutions for Real-World Environmental Cleanup. Washington, DC: ASM Press, 139–236

Qu Shengchun, Yang Haibin, Ren Dawei, et al. 1999. Magnetite nanoparticles prepared by precipitation from partially reduced ferric chloride aqueous solutions. Journal of Colloid and Interface Science, 215(1): 190–192

Rai P K. 2008. Heavy metal pollution in aquatic ecosystems and its phytoremediation using wetland plants: An ecosustainable approach. International Journal of Phytoremediation, 10(2): 133–160

Rai P K. 2010. Phytoremediation of heavy metals in a tropical impoundment of industrial region. Environmental Monitoring and Assessment, 165(1–4): 529–537

Rajesh S, Patric Raja D, Rathi J M, et al. 2012. Biosynthesis of silver nanoparticles using *Ulva fasciata* (Delile) ethyl acetate extract and its activity against *Xanthomonas campestris* pv. *malvacear-*

um. Journal of Biopesticides, 5(Suppl): 119–128

Rawat I, Kumar R R, Mutanda T, et al. 2011. Dual role of microalgae: Phycoremediation of domestic wastewater and biomass production for sustainable biofuels production. Applied Energy, 88(10): 3411–3424

Ribeiro R F L, Magalhães S M S, Barbosa F A R, et al. 2010. Evaluation of the potential of microalgae *Microcystis novacekii* in the removal of Pb^{2+} from an aqueous medium. Journal of Hazardous Materials, 179(1–3): 947–953

Salgado S G, Nieto M A Q, Simón M M B. 2006. Optimisation of sample treatment for arsenic speciation in alga samples by focussed sonication and ultrafiltration. Talanta, 68(5): 1522–1527

Schröfel A, Kratošová G, Bohunická M, et al. 2011. Biosynthesis of gold nanoparticles using diatoms—silica-gold and EPS-gold bionanocomposite formation. Journal of Nanoparticle Research, 13(8): 3207–3216

Shanab S, Essa A, Shalaby E. 2012. Bioremoval capacity of three heavy metals by some microalgae species (Egyptian isolates). Plant Signal & Behavior, 7(3): 392–399

Shankar S S, Ahmad A, Sastry M. 2003. Geranium leaf assisted biosynthesis of silver nanoparticles. Biotechnology Progress, 19(6): 1627–1631

Shankar S S, Rai A, Ahmad A, et al. 2004. Rapid synthesis of Au, Ag, and bimetallic Au Core-Ag shell nanoparticles using Neem (*Azadirachta indica*) leaf broth. Journal of Colloid and Interface Science, 275(2): 496-502

Singh R, Misra V, Singh R P. 2011. Synthesis, characterization and role of zero-valent iron nanoparticle in removal of hexavalent chromium from chromium spiked soil. Journal of Nanoparticle Research, 13(9): 4063–4073

Stengel D B, Macken A, Morrison L, et al. 2004. Zinc concentrations in marine macroalgae and a lichen from western Ireland in relation to phylogenetic grouping, habitat and morphology. Marine Pollution Bulletin, 48(9–10): 902–909

Tolles W M, Rath B B. 2003. Nanotechnology, a stimulus for innovation. Current Science, 85(12): 1746–1759

Tonon A P, Oliveira M C, Soriano E M, et al. 2011. Absorption of metals and characterization of chemical elements present in three species of *Gracilaria* (Gracilariaceae) *Greville*: a genus of economical importance. Brazilian Journal of Pharmacognosy, 21(2): 355–360

Vivek M, Kumar P S, Steffi S, et al. 2011. Biogenic silver nanoparticles by *Gelidiella acerosa* extract and their antifungal effects. Avicenna Journal of Medical Biotechnology, 3(3): 143–148

Volesky B, May-Phillips H A. 1995. Biosorption of heavy metals by *Saccharomyces cerevisiae*. Applied Microbiology and Biotechnology, 42(5): 797–806

Zhang W X. 2003. Nanoscale iron particles for environmental remediation: An overview. Journal of Nanoparticle Research, 5(3): 323–332

Zhang Guiyin, Dong Yuanyan, Li Xueyuan, et al. 2001. Effects and mechanisms of oxalate on Cd(Ⅱ) adsorbed on goethite at different pH and electrolyte concentration. Plant Nutrition and Fertilizer (in Chinese), 7(3): 305–310